Journal of Power Sources 217 (2012) 142–151

Contents lists available at SciVerse ScienceDirect

Journal of Power Sources

journal homepage: www.elsevier.com/locate/jpowsour

Effect of a nitrogen-doped PtRu/carbon anode catalyst on the durability of a direct methanol fuel cell

A.R. Corpuz [a,*], T.S. Olson [b], P. Joghee [c], S. Pylypenko [c], A.A. Dameron [b], H.N. Dinh [b], K.J. O'Neill [b], K.E. Hurst [b], G. Bender [b], T. Gennett [b], B.S. Pivovar [b], R.M. Richards [a], R.P. O'Hayre [c]

[a] Colorado School of Mines, Department of Chemistry, 1500 Illinois St, Golden, CO 80401, United States
[b] National Renewable Energy Laboratory, 1617 Cole Boulevard, Golden, CO 80401, United States
[c] Colorado School of Mines, Department of Metallurgical & Materials Engineering, 1500 Illinois St, Golden, CO 80401, United States

HIGHLIGHTS

- 645 h of MEA durability was performed on a nitrogen-doped PtRu/C anode.
- After durability, the DMFC performance of the N-doped anode is 5X the undoped anode.
- The MEA with nitrogen-doped PtRu/C performed comparably to a commercial PtRu/C.
- Nitrogen doping mitigates metal dissolution and Ru crossover during MEA durability.

ARTICLE INFO

Article history:
Received 13 March 2012
Received in revised form
1 June 2012
Accepted 3 June 2012
Available online 9 June 2012

Keywords:
Nitrogen doping
Fuel cell
Membrane electrode assembly
Platinum ruthenium
Durability
Anode

ABSTRACT

Electrochemical performance and durability of PtRu supported on N-doped Vulcan is evaluated as an anode in membrane electrode assembly (MEA) single-cell direct methanol fuel cell (DMFC) studies. This material is compared to two reference materials, an *in-house* PtRu catalyst supported on undoped Vulcan, prepared under the same conditions as the N-doped material besides doping, and a commercial PtRu/C (JM5000). Durability was tested out to 645 h, with periodic interruption for electrochemical testing. After durability, the MEA with N-doped PtRu/C retained more electrochemically active metal on the anode than the MEAs with commercial PtRu/C and undoped PtRu/C (124 compared to 106 and 82 cm^2 anode active area per cm^2 geometric surface area, respectively). From cathode CO stripping experiments and SEM-EDS studies, it was determined that the MEA with the undoped PtRu/C anode has twice as much ruthenium crossover as the MEA with the N-doped PtRu/C anode. Overall, the MEA with N-doped PtRu/C demonstrates significantly better methanol:air polarization performance compared to the MEA with undoped PtRu/C, and performs comparably to the MEA made with the commercial PtRu/C. The increase in durability for the MEA with the N-doped anode is attributed to nitrogen doping mitigating both anode metal dissolution and Ru crossover.

1. Introduction

Improving durability remains one of the most important challenges to the commercialization of direct methanol fuel cells (DMFCs) [1–8]. Durability complications arise from catalyst and membrane degradation during operation [1–3]. Catalyst degradation of standard Pt/C and PtRu/C cathode and anode catalysts respectively is often severe and irreversible, and is known to occur by metal dissolution/agglomeration (Ostwald ripening, crystal migration/coalescence, support detachment, dissolution/reprecipitation), active site contamination, and/or support corrosion [1,9]. PtRu/C anode catalysts add another complication in comparison to Pt/C cathode catalysts, as Ru crossover from the anode side to the cathode side can cause large performance loss [4].

Ru crossover has been found to occur as soon as a fuel cell is humidified, before any current generation [4]. The amount of Ru crossover needed to cause 60–70% contamination coverage on a 0.4 mg cm^{-2} Pt cathode is quite small, only 0.03 mg cm^{-2} of Ru [9]. Research in mitigating Ru crossover includes the use of hot pressing and acid treatment to pre-leach unstable Ru species, with moderate success. However, Ru crossover still occurs during current generation. Ru crossover reduces oxygen reduction kinetics on the cathode side, and has also been speculated to decrease the cathode's tolerance for methanol crossover [4]. Both accelerated

* Corresponding author. Tel.: +1 714 926 7709; fax: +1 303 273 3629.
E-mail address: april.corpuz@gmail.com (A.R. Corpuz).

0378-7753/$ – see front matter © 2012 Elsevier B.V. All rights reserved.
http://dx.doi.org/10.1016/j.jpowsour.2012.06.012

stress tests and normal DMFC operation durability studies cause crossover [4,9], and increasing Ru coverage causes a linear increase in cell performance loss [9].

In several metal-based carbon-supported electrocatalytic systems, functionalization of the carbon support has been studied as a means to ensure better anchoring of the overlying metal nanoparticles [10–24]. In particular, much work has been done functionalizing high surface area carbon with nitrogen, which was shown to improve metal dispersion and electrocatalytic activity of Pt/C catalysts [10–20]. Experimentally, nitrogen-doping has been found to provide several advantages, including decreased Pt particle size [11–13], increased Pt immobilization [25], increased electrical conductivity, increased Pt-catalyst binding energy [26,27], and increased oxygen reduction reaction (ORR) activity [11,12,14,18,28]. There is evidence that pyridinic nitrogen sites create the most attractive sites for Pt deposition and may also enhance Pt activity [12–15]. It is hypothesized that the changes in pi bonding and increased basicity afforded by a nitrogen-functionalized carbon support enhance the Pt–C bond strength and therefore are also expected to increase durability [10,11,29,30]. To a lesser extent, work has also been conducted to apply nitrogen doping to improve PtRu/C catalysts [22–24,31]. Similar effects are observed: nitrogen doping induces smaller initial PtRu particle size and improved dispersion [21–23]. Reviews on nitrogen-doped catalysts for proton exchange membrane fuel cells can be found in references [10] and [20].

There are several recently published works on nitrogen-doped Pt/C ORR and methanol oxidation reaction (MOR) durability testing [15–17,32,33], and a few on nitrogen-doped PtRu/C durability testing [31,34]. These studies found that nitrogen-doped Pt/C catalysts retained more of their initial electrochemical surface area [32], maintained smaller metal particle size [15,33], and showed smaller performance losses [15,16,33] than their undoped counterparts during durability cycling or short-term (<80 h) potentiostatic durability testing. Nitrogen-doped PtRu/C catalysts also maintained smaller metal particle size and showed smaller performance losses in comparison to their undoped counterparts during durability cycling or short-term (<80 h) potentiostatic durability testing [31,34]. Recently, our group has performed durability studies using both Pt and PtRu nanoparticle electrocatalysts sputtered on nitrogen-doped highly ordered pyrolytic graphite (HOPG) [17,31]. HOPG was chosen as a well-defined model carbon substrate to provide fundamental insight into the surface chemistry of carbon supports functionalized with nitrogen and the effect of nitrogen on the stability of Pt and PtRu nanoparticles. The durability studies using HOPG supports revealed that supports doped with relatively high amounts of nitrogen (>4%) improved the stability of PtRu nanoparticles (as evidenced by smaller changes in the coverage and particle size) and outperformed undoped supports and supports with smaller levels of nitrogen dopant. It was hypothesized that pyridinic nitrogen sites as well as multi-nitrogen defects may be responsible for the differences in behavior [31]. Recently, Kondo, Suzuki, and Nakamura found that Pt on N-doped HOPG maintained catalytic activity during cycling of the H_2-D_2 exchange reaction, unlike undoped and Ar-doped counterparts. This was attributed to the fact that Pt on N-doped HOPG maintained a monolayer morphology during cycling, while Pt on unmodified HOPG grew from monolayers to multilayers [35].

In the present work, in order to examine the effects of a nitrogen-functionalized carbon support in a real DMFC environment, we have deployed a high surface-area catalyst consisting of PtRu sputtered on N-doped carbon powder in the anode of a single-cell DMFC membrane electrode assembly (MEA). We compare its performance to that of MEAs fabricated using an otherwise identical undoped control anode catalyst as well as a standard commercial benchmark anode catalyst under long term (>600 h) durability testing with periodic interruption for detailed anode and cathode CO stripping and linear-sweep voltammetry methanol polarization measurements in order to monitor the evolution of all three MEAs. Nitrogen doping of Vulcan black was done using ion implantation, which at low ion implantation dosages allows implantation of nitrogen within the near-surface region of the carbon while minimizing implant damage [17]. This technique allows introduction of nitrogen functionalities such as pyridinic, graphitic and pyrrolic nitrogen into carbon-based structures such as carbon blacks [36,37] and HOPG, a model substrate employed in the study of the stability of supported PtRu [21,31]. Sputtering was done from a single alloyed 50:50 PtRu target in an *in-house* system that allows ion implantation and sputtering to be done back-to-back. While short-term (80 h) durability testing of a nitrogen-doped PtRu/C MEA has been published [23], at the time of writing, this work is the first report known to the authors on long-term durability testing (>500 h) of a nitrogen-doped PtRu/C MEA [38]. This paper therefore provides valuable and definite evidence on the long-term durability benefits of a nitrogen-doped PtRu/C anode catalyst in an operating DMFC MEA.

2. Experimental

PtRu on unmodified (undoped) carbon and PtRu on a nitrogen-doped carbon were made *in-house* using a UHV vacuum chamber equipped with an orthogonally oriented 2″ sputter gun (Onyx Mag 2, Angstrom Sciences, Duquesne, PA), an ion source (3 cm DC (ITI) ion gun, Veeco, Santa Barbara CA), positioned at 35° from normal to the powder surface, and a powder sample holder ("wheel") rotated at 30 rpm to allow for agitation of powder sample. For the N-doped PtRu/C, nitrogen doping of 500 mg of commercially available carbon powder (Cabot Vulcan XCR72R) was done by ion implantation at room temperature with a non-mass separated nitrogen ion beam. The ion beam energy used was 100 eV, with a beam current of 13 mA, with an implantation time of 60 min. The range is due to losses of powder in the chamber and uncertainties in surface area and uniform implantation. PtRu was incorporated onto either the unmodified Vulcan or N-doped Vulan by magnetron sputtering from a 50:50 PtRu alloy target. Sputtering was done at 25 mTorr with DC power of 45 W, using argon as the sputter gas with 10 mol% O_2, for 60 min. The custom sputter chamber is described in detail elsewhere [39]. For the N-doped PtRu/C, ion implantation and sputtering were done back-to-back in the same chamber without breaking vacuum.

Before MEA preparation, several techniques were used to determine metal loading and composition of the powders. Initial composition of the *in-house* materials was measured by X-ray fluorescence (XRF) using a maXXi 5/PIN (Roentgen Analytic) with a tungsten target. The XRF composition was obtained by comparison to a calibrated $Pt_{1-x}Ru_x$ standard using software provided by the XRF manufacturer. Thermogravimetric analysis (TGA) was used to determine the total metal content of the PtRu/C powders. A TA Q600 (TA Instruments, New Castle, DE) was used with 100 mL min^{-1} of synthetic air (80% N_2, 20% O_2). The heating rate was 5 °C min^{-1} to 850 °C. We assume the final mass at 850 °C is composed of RuO_2 and Pt. X-ray Photoelectron Spectroscopy (XPS) analysis of the synthesized catalysts was done on a Kratos Nova XPS with a monochromatic Al K-alpha source operated at 300 W. Data analysis was performed using CasaXPS software and included subtraction of the linear background for O 1s and N 1s. The Shirley background was used for Pt 4f, Ru 3p, and combined C 1s/Ru 3d regions and charge referencing was done using the graphitic peak at 284.6 eV. Details on the curve-fitting procedure can be found elsewhere [31].

MEAs (5 cm^2 active area) using both the N-doped and undoped *in-house* anode catalysts, as well as a commercial (control) anode catalyst (HiSPEC 5000 PtRu/C, Johnson Matthey, Inc.) were made by the hand-painting method. In each case, the respective anode catalyst ink, comprised of 23 mg catalyst, 320 mg 5 wt% Nafion in alcohol, and 300 mg water, was painted onto a Nafion 117 membrane over a vacuum table at 70 °C. After drying, the catalyst coated membrane was hot-pressed at 130 °C and 294 lbs for 10 min. During the cell assembly, a Johnson Matthey gas diffusion electrode (GDE), which includes both a gas diffusion layer (GDL) and catalyst, with Pt loading of 0.4 mg cm^{-2} was placed on the cathode side of the MEA. A GDL made of carbon coated carbon paper (SGL GDL 25BC) was placed on the anode side of the MEA.

Metal electrochemical surface areas were determined individually for each of the anodes and cathodes by CO stripping prior to durability testing and then at periodic intervals during the durability testing. 300 sccm of 1% CO in Ar at 100% relative humidity (RH) was flowed for 30 min on the side of interest (anode or cathode) followed by 300 sccm of N_2 at 100% RH for 30 min before each CO stripping test. On the other side (cathode or anode), 100 sccm of 100% RH H_2 was flowed; this was used as a reference dynamic hydrogen electrode (DHE). After these fuel flows, a cyclic voltammogram (CV) between 0.1 V and 0.9 V vs. DHE was taken for 3 cycles. During CV measurements, the fuel flow was 0 sccm on the side of interest (anode or cathode) and 50 sccm of H_2 on the other side (cathode or anode).

Methanol anode polarization curves were collected using a linear-sweep voltammogram (LSV) by feeding 1 M methanol at the flow rate of 1 mL min^{-1} to the anode side and by purging H_2 (100% RH) at the flow rate of 50 sccm to the cathode of the MEA. LSV testing was carried out using a potential sweep in the range from 0 to 0.7 V vs DHE at a scan rate of 2 mV s^{-1}. Data between 0.2 and 0.6 V was used. Methanol anode polarization curves were obtained at the onset of durability testing as well as at periodic intervals during the durability testing.

DMFC durability testing was conducted by maintaining a constant cell voltage of 0.4 V for a total of 645 h for all three MEAs (N-doped PtRu/C, undoped PtRu/C, and commercial PtRu/C, respectively). 0.4 V is a typical operating voltage and is an efficient operating point; one of the longest reported single-cell DMFC life tests is done under similar conditions, held at 0.4 V [40]. Fuel feed was 1 M methanol (0.7 ml min^{-1}) and 100% RH air (3.3 stoichiometric flow, 60 sccm minimum flow) to the anode and cathode, respectively, at 80 °C. At various intervals, durability testing was interrupted to take performance curves, CO stripping CVs, and methanol anode polarization LSVs. The measurement time associated with these tests was not included in the total elapsed durability testing time for the three MEAs. The DMFC performance curves were collected with the same fuel feed rates described for durability testing. The DMFC performance curves were collected galvanostatically by altering the current mode at steps of 15 min and recording the corresponding voltages. The voltage values recorded for the last 5 min at each current step were averaged and used for plotting the DMFC polarization curves.

Elemental compositions of the anode and cathode in post-durability MEAs were evaluated using a JEOL JSM-7000F Field Emission Microscope (SEM) with EDAX Genesis Energy Dispersive X-ray (EDX) Spectrometer. MEA cross-sections were prepared by immersion in liquid nitrogen and sectioning with a razor blade.

3. Results and discussion

As shown in Table 1, the undoped PtRu/C, N-doped PtRu/C, and commercial PtRu/C powders have approximately 30 wt% of 1:1 PtRu on carbon. Based on XPS analysis, the *in-house* materials are a mix of anhydrous and hydrous oxides, and the distribution of ruthenium in the two *in-house* materials is very similar. The commercial PtRu/C, on the other hand, also has a significant amount of metallic ruthenium in addition to oxide species. There is a small amount of nitrogen in the undoped PtRu/C and commercial PtRu/C, associated with a narrow XPS nitrogen peak, whereas the nitrogen spectra of the N-doped PtRu/C are much wider and similar to N-doped HOPG substrates [21], indicating the presence of multiple nitrogen functionalities, including pyrrolic, pyridinic, amine and graphitic N.

Table 1
Elemental composition of powders.

Catalyst:	Undoped PtRu/C	N-doped PtRu/C	Commercial PtRu/C
Platinum, wt%[a]	18	21	18–21[b]
Ruthenium, wt%[a]	11	9	9–11[b]
Platinum, at% (of total metal)[a]	47	56	47–53[b]
Ruthenium, at% (of total metal)[a]	53	44	47–53[b]
XPS data			
C 1s	89.0	89.0	89.2
O 1s	9.0	6.9	7.8
Pt 4f	1.5	1.5	1.2
Ru 3p	1.9	1.7	1.3
N 1s	0.2	1.0	0.6
Ru1, %Ru metallic	0.0	0.0	10.7
Ru2, %RuO_2 screened final state	6.6	9.8	32.1
Ru2, %$RuO_2 \cdot nH2O$	56.1	53.9	38.7
Ru3, %RuO_2 unscreened final state	37.3	36.3	18.6

[a] Total metal weight percent of PtRu on carbon is measured by TGA. Pt:Ru ratio is determined by XRF.
[b] Data as given by the manufacturer, Johnson Matthey.

Fig. 1 shows the initial electrochemical characteristics for the MEAs with undoped PtRu/C, N-doped PtRu/C, and commercial PtRu/C anodes of approximately the same metal loading (1 mg cm^{-2}). CO stripping of the anode side can be found in Fig. 1a. The undoped PtRu/C anode exhibits a single CO stripping peak with the highest electrochemically active surface area (ECSA), measuring 0.204 m^2 (408 cm^2 of ECSA per cm^2 of geometric area). The commercial PtRu/C CO stripping peak is bimodal, with an ECSA of 0.143 m^2 (286 cm^2 of ECSA per cm^2 of geometric area). The smaller peak at higher potential can be attributed to a Pt-only phase [4,41,42]. The N-doped PtRu/C exhibits a single, narrow peak with the lowest ECSA, measuring 0.108 m^2 (216 cm^2 of ECSA per cm^2 of geometric surface area). The fact that the N-doped PtRu/C has the lowest ECSA will be discussed in more detail later in this section.

Fig. 1b provides methanol anode polarization curves comparing the raw anode performances. The undoped PtRu/C and N-doped PtRu/C anodes perform moderately better than the commercial PtRu/C. At 0.4 V, the undoped PtRu/C and N-doped PtRu/C anodes both generate 0.145 A cm^{-2}, higher than the 0.111 A cm^{-2} generated by the commercial PtRu/C. When the methanol anode polarization curves are normalized to ECSA, as shown in Fig. 1c, the N-doped PtRu/C anode shows much better performance (6.66 A m^{-2} at 0.4 V) than both the undoped PtRu/C and commercial PtRu/C (3.58 A m^{-2} at 0.4 V for both anodes). The same trend is found when comparing the anodes using methanol:air performance data, found in Fig. 1d and e. When comparing raw current, as shown in Fig. 1d, all three MEAs perform similarly. After normalizing to ECSA, as shown in Fig. 1e, the MEA with N-doped PtRu/C generates higher current for a given voltage in comparison to the MEA with undoped PtRu/C and the MEA with commercial PtRu/C. Refer to Table 2 for a complete summary of the electrochemical performance for the three MEAs (both initial and over the course of durability testing). The fact that

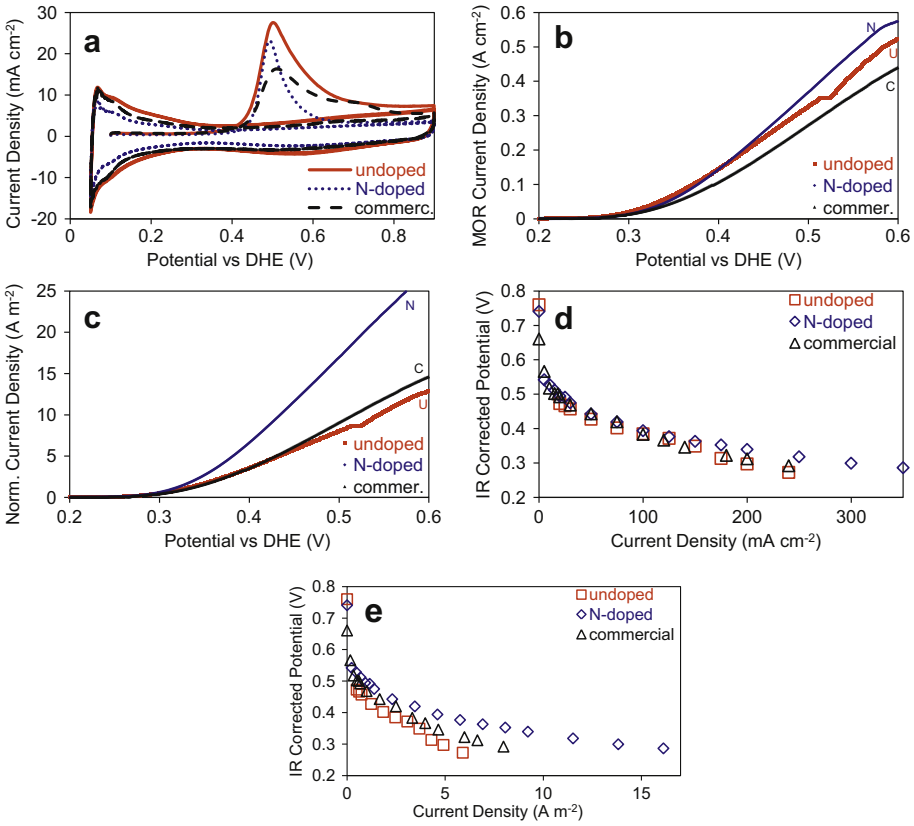

Fig. 1. Initial electrochemical studies of the MEAs with undoped PtRu/C, N-doped PtRU/C, commercial PtRu/C (HiSpec 5000), consisting of a) CO stripping on the anode of the MEAs at 20 mV/s, b) raw methanol anode polarization curves, c) Methanol anode polarization normalized to ECSA, d) raw methanol:air performance curves, and e) methanol:air performance curves normalized to ECSA. On 1b and 1c, U stands for undoped PtRu/C, N is N-doped PtRu/C, and C is commercial PtRu/C.

the methanol anode polarization curves and the methanol:air performance curves show the same initial trend between the three MEAs is not surprising as all three MEAs utilized nominally identical commercial cathodes.

As stated before and shown in Fig. 1a, the N-doped PtRu/C has a smaller electrochemical surface area than the undoped PtRu/C and the commercial PtRu/C. Generally, other works have shown that smaller particle sizes and higher ECSA are obtained when metal is deposited through routes that depend on nucleation site density, specifically wet chemical preparation of Pt on N-doped carbons [11,12,14,18,28]. In this work, we used sputtering to make the PtRu nanoparticles, which is not as sensitive as wet chemical preparation and has no preferential nucleation sites, therefore an increase in ECSA is not expected. However, this does not explain the decrease in ECSA with nitrogen-doping, and we surmise that the method of nitrogen doping by ion implantation plays a role in the decrease of ECSA by possibly modifying the carbon surface morphology (more investigation is needed). Even with lowered ECSA, the N-doped PtRu/C shows the same raw performance as the undoped PtRu/C, and demonstrates better performance than the commercial catalyst (Fig. 1b, d). We hypothesize that the ability to incorporate nitrogen while increasing (or at least without decreasing) the ECSA would allow further gains in absolute methanol oxidation activity.

Durability testing on each of the three MEAs was done by holding each cell at 0.4 V under DMFC operation conditions for a total of 645 h, shown in Fig. 2, with periodic stops for CO stripping and methanol anode polarization studies. Fig. 3 provides CO stripping curves for the undoped PtRu/C, N-doped PtRu/C, and commercial PtRu/C anodes as a function of operation time during the durability test. For the MEA with the undoped PtRu/C anode (Fig. 3a), very narrow single CO stripping peaks are observed until a clear splitting of the CO stripping peak occurs at 323 h (although the data is not shown here, splitting of the CO stripping peak was in fact first observed at 290 h). This peak splitting, which is often observed in PtRu DMFC catalysts subjected to long-term durability testing, indicates the formation of separate phases of Pt and Ru within the anode [4,41,42]. This phase separation is most likely caused by loss of Ru from the anode, a result that is corroborated by the cathode CO stripping results shown later. In marked contrast to the undoped *in-house* PtRu/C anode catalyst, the N-doped PtRu/C anode catalyst maintains a single narrow CO stripping peak even after 645 h of durability testing (Fig. 3b). This suggests that a single-phase PtRu alloy is retained in the N-doped PtRu/C anode throughout the entirety of the durability study. As has been suggested by our prior HOPG-based work on N-doped PtRu/C catalysts [31], the presence of nitrogen functional groups in the catalyst support likely plays a key role in protecting the single phase PtRu alloy by decreasing Ru loss. Unlike both the undoped and N-doped PtRu/C catalysts, the commercial PtRu/C (HiSpec 5000) anode catalyst shows two broad CO stripping peaks even during the initial stage of testing (Fig. 3c). The two broad peaks slowly diminish and reduce to a single broad peak after increasing operational time under the durability testing protocol. We hypothesize that this behavior may be due to the presence of higher initial amounts of a separate phase of Ru in the commercial catalyst which is then preferentially leached out during the durability test, leaving a non-distinct distribution of PtRu alloys with varying Ru composition at later times. As shown in the XPS data in Table 1, initially the commercial PtRu/C has a metallic ruthenium phase that is not observed in the *in-house* materials.

Quantitative information extracted from the anode CV stripping tests is summarized in Fig. 4a, which provides the relative ECSA

Table 2
Methanol oxidation current density tables, values taken at 0.4 V.

Durability (h)	MAP (mA cm^{-2})[a]	Anode ECSA (m^2)	MAP (A m^{-2})[b]
Undoped PtRu/C			
0	154	0.20	3.8
54	153	0.15	5.3
122	129	0.14	4.6
187	113	0.12	4.6
232	44	0.11	2.1
290	69	0.093	3.7
323	82	0.096	4.3
583	82	0.084	4.9
645	77	0.041	9.4
N-doped PtRu/C			
0	144	0.11	6.6
54	128	0.098	6.5
122	130	0.091	7.1
222	100	0.082	6.1
323	83	0.077	5.4
583	65	0.076	4.3
645	84	0.062	6.8
Commercial PtRu/C			
0	108	0.15	3.6
54	115	0.082	7.0
122	85	0.085	5.0
187	85	0.078	5.4
232	83	0.074	5.6
290	85	0.065	6.5
323	94	0.060	7.8
583	85	0.059	7.2
645	97	0.053	9.1

[a] Current from methanol anode polarization at 0.4 V, normalized by geometric surface area (5 cm^2 for all data). Anode polarization curves collected by feeding 1 M methanol (1 mL min^{-1}) to anode and H_2 to cathode (50 sccm) at 80 °C and at a scan rate of 2 mV s^{-1}.

[b] Current density from methanol anode polarization at 0.4 V, normalized by PtRu ECSA. Anode polarization curves collected by feeding 1 M methanol (1 mL min^{-1}) to anode and H_2 to cathode (50 sccm) at 80 °C and a scan rate of 2 mV s^{-1}.

estimates obtained for the three anode catalysts as a function of durability testing time. The ability of the N-doped carbon catalyst to mitigate ECSA loss (including less metal dissolution and improved Ru retention) is clearly evident in these ECSA trends, which show that the relative ECSA loss in the N-doped PtRu/C anode catalyst is significantly less (by a factor of 2–3X) than in the undoped PtRu/C and commercial PtRu/C catalyst counterparts. In absolute terms, after 645 h of durability, the N-doped PtRu/C anode still had

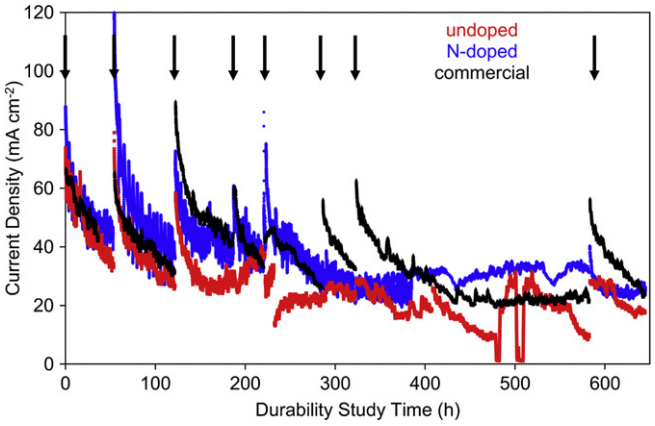

Fig. 2. Durability study of undoped PtRu/C (light gray), N-doped PtRu/C (dark gray), and commercial PtRu/C (HiSpec 5000) (black). Arrows denote the times at which the durability study was stopped and other testing (CO stripping, methanol anode polarization, methanol:air polarization) was done. Areas where the current goes to zero indicate methanol delivery failure due to occasional power loss to the lab.

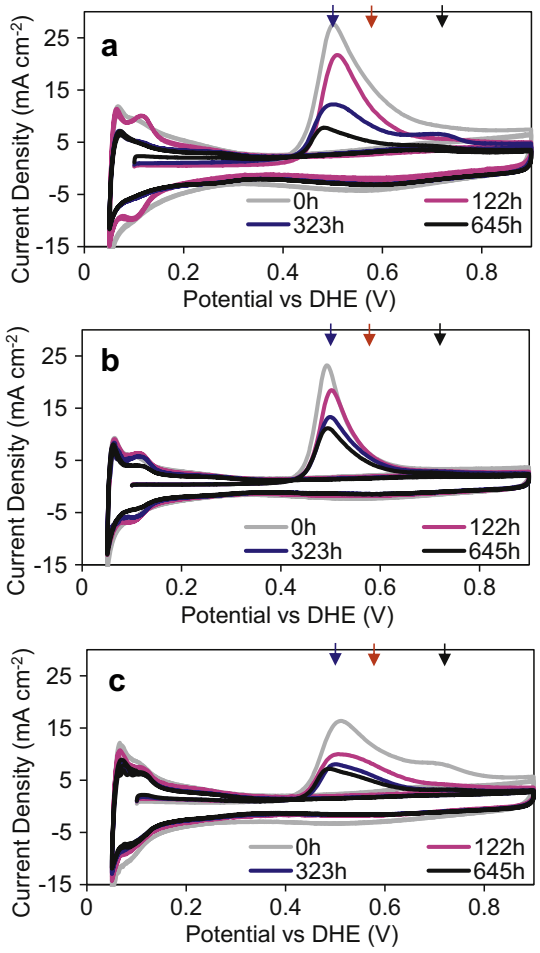

Fig. 3. CO stripping on the anode of the MEAs with a) undoped PtRu/C, b) N-doped PtRu/C, and c) commercial PtRu/C (HiSpec 5000) at 20 mV s^{-1}. The arrows from right to left (0.72 V, 0.58 V, 0.50 V) denote where the CO stripping peaks of pure Pt, pure Ru, and Pt:Ru alloy of 1:1 atomic ratio are expected to be at 20 mV s^{-1} respectively [39].

0.062 m^2 (124 cm^2 of anode ECSA per cm^2 of geometric area) of electrochemically active surface area left on it, while the commercial and undoped PtRu/C anodes had 0.053 and 0.041 m^2 (106 and 82 cm^2 of anode ECSA per cm^2 of geometric area, respectively) of retained electrochemically active surface area respectively. Considering that the N-doped PtRu/C anode initially had the least amount of electrochemically active surface area, the trends in ECSA indicate that nitrogen doping facilitates ECSA retention during durability.

Fig. 5 provides cathode CO stripping curves for the MEAs containing the undoped PtRu/C, N-doped PtRu/C, and commercial PtRu/C anodes respectively as a function of operation time during the durability test. All three MEAs employed the same pure Pt/C commercial cathode catalyst (0.4 mg cm^{-2} Pt, no Ru). For all three MEAs, the initial cathode CO stripping curves show a single peak around 0.7 V which can be clearly attributed to Pt. However, during durability studies, the cathodes of all three MEAs are affected by Ru crossover (the Ru is coming from the anode side), and a new peak appears at around 0.55 V due to Ru. Nevertheless, there are clear differences in the time-onset and magnitude of this Ru peak for the three MEAs. For the cathode of the MEA with undoped PtRu/C, the CO oxidation peak due to the presence of Ru grows bigger than the peak for Pt even after a relatively short durability testing period of 122 h, as shown in Fig. 5a (although the data is not shown here, a larger Ru peak in comparison to the Pt peak was in fact first

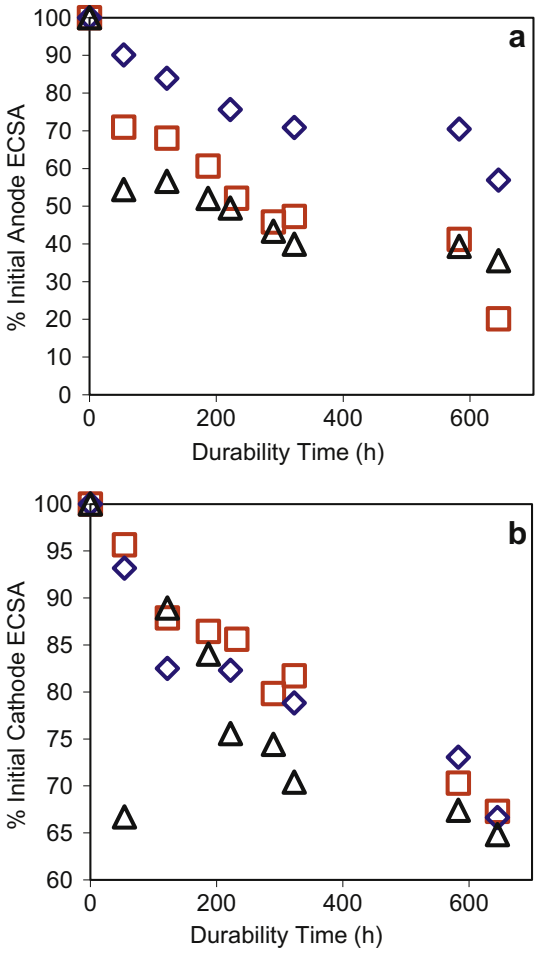

Fig. 4. Relative amount of ECSA as a function of durability for the (a) anode side and (b) cathode side for the MEAs containing undoped PtRu/C (diamond data points), N-doped PtRu/C (square data points), and commercial PtRu/C (triangle data points) anodes.

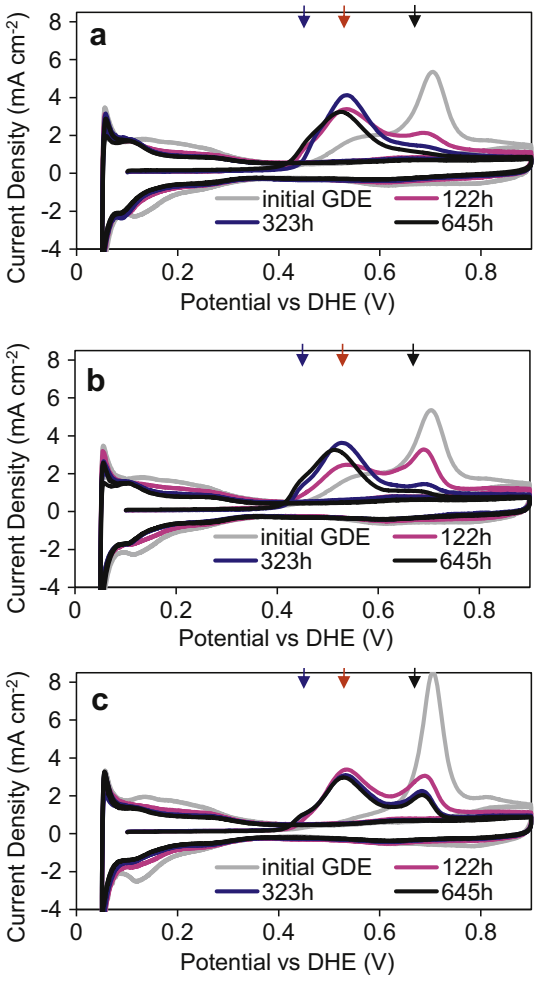

Fig. 5. CO stripping on the cathode of the MEAs with a) undoped PtRu/C, b) N-doped PtRu/C, and c) commercial PtRu/C (HiSpec 5000) at 5 mV s^{-1}. The arrows from right to left (0.67 V, 0.53 V, 0.45 V) denote where the CO stripping peaks of pure Pt, pure Ru, and Pt:Ru alloy of 1:1 atomic ratio are expected to be at 5 mV s^{-1} respectively [39].

observed at 54 h). A similar phenomenon is observed for the cathode of the MEA with commercial PtRu/C (Hi-spec 5000) after the durability testing reaches 122 h (Fig. 5c). For the cathode of the MEA with N-doped PtRu/C (Fig. 5b), the CO oxidation peak due to the presence of Ru becomes larger than the peak for Pt only after 222 h of durability testing (not shown in figure). After 645 h of durability testing, the cathode CO stripping curves for the MEAs with undoped PtRu/C and N-doped PtRu/C look similar, with the N-doped PtRu/C MEA retaining a little more of the pure Pt peak than the undoped PtRu/C MEA. This is corroborated by the data from the post-mortem SEM-EDS studies shown in Table 3, Fig. 7, and Fig. 8 providing evidence for ruthenium on the cathode side. From SEM-EDS, direct quantification of the amount of Ru crossover for each MEA is also obtained. The cathode of the MEA with N-doped PtRu/C had 6.6% Ru metal atomic percent, while the cathode of the MEA with undoped PtRu/C had 11.3% Ru metal atomic percent. Since the cathode sides started with no Ru, these numbers indicate twice higher levels of ruthenium crossover in the undoped material as compared to its N-doped counterpart. This data comparing the MEAs with N-doped PtRu/C and undoped PtRu/C provides further support that nitrogen doping suppresses ruthenium crossover from the anode side to the cathode side.

As shown in Fig. 5c, the MEA with commercial PtRu/C has a more well-defined Pt peak in its cathode CO stripping curve at 645 h than the MEAs made from the *in-house* anodes. Again, this is corroborated by the data from the post-mortem SEM-EDS studies (Table 3). The cathode of the MEA with commercial PtRu/C had only 4.1% Ru metal atomic percent and 95.9% Pt metal atomic percent. We believe that the differences in the cathode metal after 645 h between the MEAs with commercial PtRu/C and *in-house* PtRu/C anodes are related to initial differences in anode metal compositions. As shown in the XPS data from Table 1, the commercial PtRu/C anode has metallic ruthenium and different amounts of ruthenium oxide species than the *in-house* anodes. We hypothesize that the ruthenium species on the commercial PtRu/C are more likely to dissolve without redepositing on the cathode side in comparison to the ruthenium species on the *in-house* catalysts (as the undoped and N-doped PtRu/C have similar ruthenium species and compositions). This would explain the fact that the MEA with commercial PtRu/C had only 4.1% Ru metal atomic percent on the cathode yet a 64.4% loss of anode ECSA (Fig. 4a) after 645 h.

Quantitative information extracted from the cathode CV stripping tests is summarized in Fig. 4b, which provides the relative ECSA estimates obtained for the MEAs with the three different anode catalysts but same cathode catalyst as a function of durability testing time. For all three MEAs, Fig. 4b shows a decrease in % of initial cathode ECSA, followed by an increase, then followed by another decrease. Also, overall the relative cathode ECSA decreases with durability testing time, but much more slowly than the anode

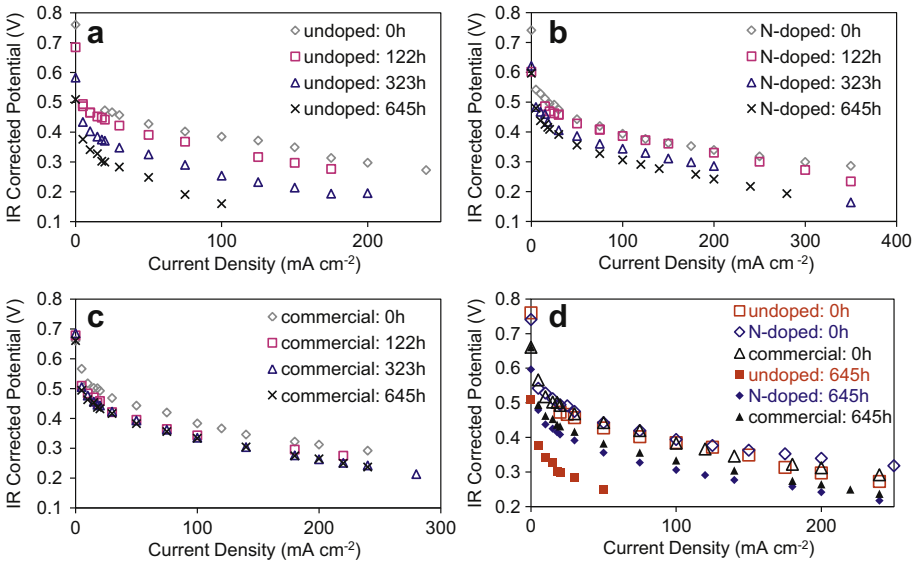

Fig. 6. Comparison of initial DMFC performances and post-durability testing DMFC performances for different time periods for the MEAs with a) undoped PtRu/C, b) N-doped PtRu/C, and c) commercial PtRu/C (HiSpec 5000). d) Comparison of DMFC performances of all the MEAs after the period of 0 and 645 h.

ECSA. These trends are due to competing platinum ECSA loss during durability and ruthenium crossover adding metal to the cathode side from the anode side. After crossover, ruthenium ECSA can be lost from the cathode side as well. The MEA with undoped PtRu/C and the MEA with N-doped PtRu/C have nearly the same total ECSA loss on the cathode after 645 h. However, as stated before, the post-mortem SEM-EDS analysis shows a larger Pt:Ru ratio for the undoped PtRu/C anode than the N-doped PtRu/C anode. These results are consistent with the findings from the anode CO stripping presented in Fig. 3 and reinforce the conclusion that nitrogen functionalization of the carbon support helps to reduce both the loss of electrochemically active surface area, and more specifically, the loss of Ru, from supported PtRu anode catalyst nanoparticles in an operating fuel cell environment.

Along with ruthenium crossover, methanol crossover is a major concern of MEA degradation during operation. The major factors in methanol crossover are membrane structure and morphology, membrane thickness, and fuel cell operating conditions [43]. To minimize any differences due to methanol crossover between the 3 MEAs that we tested, all MEAs were made with the same membrane, Nafion 117. Additionally, Nafion 117 is considered a relatively thick membrane (0.007 inches), so methanol crossover should occur to a lesser extent. Also, all three MEAs started with the same commercial cathode, so all three MEAs should start with the same initial methanol intolerance on the cathode side.

Fig. 6 compares the DMFC performance (methanol:air) for the MEAs containing the undoped PtRu/C, N-doped PtRu/C, and commercial PtRu/C anodes respectively as a function of operation time during the durability test. From Fig. 6d, it is apparent that before durability testing the MEAs with undoped PtRu/C, N-doped PtRu/C, and commercial PtRu/C exhibit comparable performance.

Table 3
Atomic percents of total metal content from post-mortem SEM-EDS analysis.

Anode catalyst material	Anode composition[a]		Cathode composition[a]	
	Pt, at%	Ru, at%	Pt, at%	Ru, at%
Commercial PtRu/C	59.2 ± 2.2	40.8 ± 2.2	95.9 ± 0.8	4.1 ± 0.8
Undoped PtRu/C	65.9 ± 1.4	34.1 ± 1.4	88.7 ± 0.9	11.3 ± 0.9
N-doped PtRu/C	64.7 ± 0.9	35.3 ± 0.9	93.4 ± 0.3	6.6 ± 0.3

[a] Atomic percent of total metal content, as determined by five measurements.

However, after 645 h of durability testing, the N-doped PtRu/C shows a considerably higher performance than the undoped PtRu/C, and similar performance to the commercial PtRu/C. After 645 h of durability testing, the MEA with N-doped PtRu/C still shows 25 mA cm^{-2} at 0.4 V (IR corrected), much higher than the 5 mA cm^{-2} exhibited by the MEA with undoped PtRu/C. On correlating these results with those from CO stripping and methanol anode polarization, we infer that N-doping in the carbon substrate can reduce ruthenium crossover from the anode to the cathode, which, in turn, slows the destruction of the cathode active sites from ruthenium crossover and hence enables the N-doped MEA to maintain higher DMFC performance.

Overall, the MEA with N-doped PtRu/C has comparable methanol:air performance and methanol anode polarization performance as the MEA with commercial PtRu/C after 645 h of durability. However, the reasons for their good durability in comparison to the MEA with undoped PtRu/C are different. The MEA with N-doped PtRu/C shows decreased metal dissolution, as it starts with a relatively low anode ECSA but has the highest anode ECSA after 645 h of durability. This is not the case with the MEA with commercial PtRu/C, which loses much of its initial electrochemical surface area (Fig. 4a). Despite its large loss of anode metal, not very much (relatively) of the ruthenium from the commercial PtRu/C anode is redeposited on the cathode, as shown by the cathode CO stripping (Fig. 5c) and post-mortem SEM studies (Table 3). This behavior may be explained by the initial composition of the ruthenium species on the commercial PtRu/C (XPS data, Table 1). It started with more metallic ruthenium than either the N-doped or undoped PtRu/C, which may oxidize during durability and/or be less likely to redeposit on the cathode side.

We can compare loss in anode ECSA to overall power density loss for the three MEAs. After 645 h of durability, the N-doped PtRu/C anode ECSA decreased from 216 cm^2 of anode ECSA per cm^2 of geometric area at 0 h to 124 cm^2 cm^{-2} at 645 h, the commercial PtRu/C anode ECSA decreased from 286 cm^2 cm^{-2} at 0 h to 106 cm^2 cm^{-2} at 645 h, and the undoped PtRu/C anode ECSA decreased from 408 cm^2 cm^{-2} at 0 h to 82 cm^2 cm^{-2} at 645 h. This corresponds to an ECSA loss of 43% for the N-doped PtRu/C anode over the 645 h, 63% for the commercial PtRu/C anode, and 80% for the undoped PtRu/C anode. Calculating the power density losses at 50 mA cm^{-2} before and after durability gives 20%, 14%, and 42% for

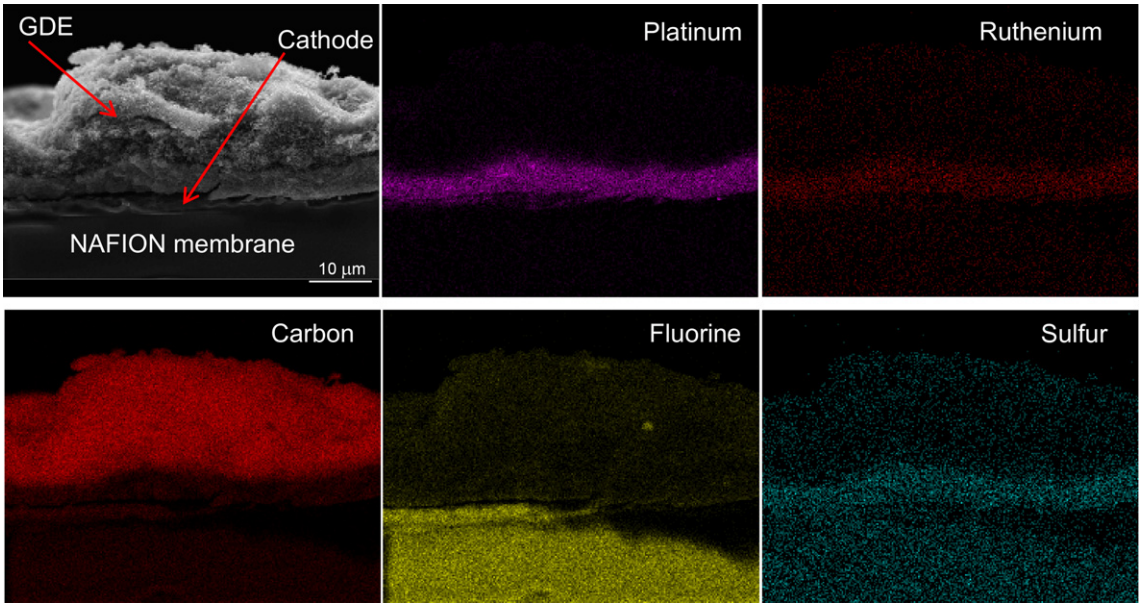

Fig. 7. EDS mapping of the cathode in the post-cycled MEA with undoped PtRu/C.

the MEA with N-doped PtRu/C, commercial PtRu/C, and undoped PtRu/C respectively. For the N-doped and undoped PtRu/C, the ECSA loss and power density loss seem very relatable; for every 10% of ECSA anode loss, there is 5% power density loss. However, the trend is not the same for the commercial PtRu/C; at 63% ECSA anode loss, there is only 14% power density loss. We believe this difference is due to the lessened ruthenium crossover in the MEA with the commercial anode, which, in turn, we attribute to the difference in

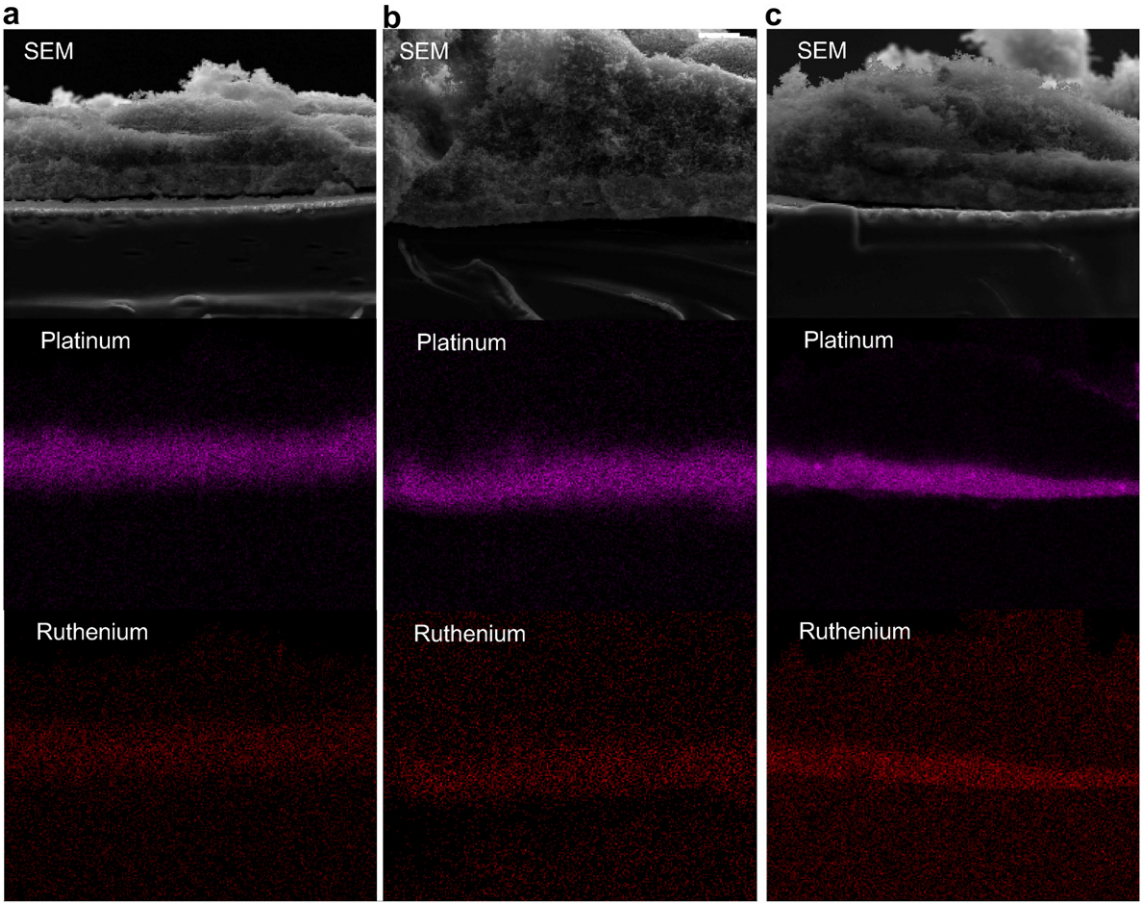

Fig. 8. EDS mapping of the cathode in post-cycled MEAs with the following anodes: a) undoped PtRu/C, b) N-doped PtRu/C, and c) commercial PtRu/C, JM 5000. Broadening of the Pt and Ru bands in a) and b) is associated with drift during acquisition of EDS maps.

initial ruthenium species. As mentioned earlier, the *in-house* undoped and N-doped PtRu/C started with very similar ruthenium species profiles, while the commercial PtRu/C started with much more metallic ruthenium and less ruthenium oxides. The ruthenium species on the commercial anode may be more stable and less susceptible to dissolution and reprecipitation on the cathode side.

Barring carbon corrosion (since high cathode potentials were avoided), there are two sintering mechanisms that can account for decreased ECSA during operation, one being dissolution and reprecipitation and the other being migration and coalescence [1]. Other work with Pt systems has shown evidence of superimposition of these two mechanisms during durability [1,44,45]. The presence of ruthenium on the cathode side unambiguously supports dissolution and reprecipitation as a mechanism for ECSA loss on the anode side. Post-mortem SEM (Figs. 7 and 8) also show some platinum and ruthenium in both the membrane and diffusion layers, providing further evidence for dissolution and reprecipitation as a mechanism for ECSA loss. These finding are consistent with those of Ferreira et al., where Pt was found near the cathode-membrane interface. Here, Ru crossover and metal deposition was found in all MEAs, including the MEA with the nitrogen doped anode, although Ru crossover was slower in the nitrogen-doped MEA. From these results, it can be inferred that nitrogen doping slows the dissolution and reprecipitation mechanism but does not stop it completely. In a previous work, a model carbon system consisting of PtRu on unmodified highly ordered pyrolytic graphite (HOPG) was compared to PtRu on nitrogen-doped HOPG (N-HOPG). TEMs before and after electrochemical durability cycling were taken of these model systems. It was found that the PtRu particle sizes on the unmodified HOPG increased greatly after durability cycling (from an average particle size of approximately 2 nm–11 nm), including large particle agglomerations. This supports nanocrystalline migration and coalescence as a mechanism for reduced electrochemical surface area. On the other hand, PtRu particle sizes on the N-HOPG did not increase nearly as much (from an average particle size of approximately 1.5 nm–2.3 nm) and did not show much particle agglomeration. This suggests that nitrogen-doping dramatically reduces ECSA loss due to migration and coalescence. Combining these studies, we hypothesize that the main benefit of nitrogen-doping is minimization of migration and coalescence, and while it slows dissolution and reprecipitation, it does not stop it completely. This may be explained by increased metal–support interaction afforded by nitrogen doping [10,11,29,30]. Since a nitrogen atom has an additional electron in comparison to a carbon atom, nitrogen incorporated into a carbon network will increase electron density in that network. This, in turn, should increase the metal-catalyst binding energy [26,27] and prevent sintering and agglomeration of particles. Conceptually, nitrogen doping should decrease migration and coalescence more than dissolution and reprecipitation as metal atoms not near the nitrogen-doped support will be less affected by the increased electron density in the support. To further elucidate the mechanism of ECSA loss, a paper detailing the use of transmission electron microscopy and *in-situ* small angle X-ray scattering to determine and compare particle sizes during durability cycling on PtRu/C and N-doped PtRu/C powders is forthcoming.

4. Conclusion

In initial methanol:air performance, the MEA with the N-doped PtRu/C performed similarly to the undoped PtRu/C and commercial PtRu/C, despite its having the lowest ECSA. The N-doped and undoped *in-house* PtRu/C anodes had better initial methanol anode polarization performance than the commercial PtRu/C. We speculate that this is due to the *in-house* catalysts having a higher concentration of hydrous ruthenium oxide species than the commercial catalyst, which has been shown to be the preferred species for DMFC [46]. When normalized to ECSA, the N-doped PtRu/C exhibits superior methanol oxidation performance than undoped PtRu/C and commercial PtRu/C of similar metal loading. If it is possible to achieve nitrogen doping without decreasing ECSA, this may lead to very high activity catalysts in the future.

By examining CO stripping on the anode as a function of durability testing, it is observed that the N-doped PtRu/C anode demonstrates a narrower and longer-lived single-phase PtRu alloy distribution than either the undoped PtRu/C or the commercial PtRu/C anode catalysts, and also shows a greatly reduced rate of anode ECSA loss during durability testing. Even though it starts with the lowest amount of anode ECSA initially, the N-doped PtRu/C has the highest amount of anode ECSA after 645 h of durability testing in comparison to both the undoped PtRu/C and commercial PtRu/C. This result, in combination with the post-mortem SEM-EDS studies, suggests that nitrogen doping decreases metal dissolution during operation. Furthermore, CO stripping on the cathode as a function of durability testing indicates that ruthenium crossover with the N-doped PtRu/C anode is reduced in comparison to the undoped PtRu/C. These combined effects greatly impact the methanol:air polarization performance as a function of operating time, with the N-doped PtRu/C showing significantly lower performance loss during long-term operation than the undoped PtRu/C.

Acknowledgements

Work at CSM supported by the Army Research Office under grant #W911NF-09-1-0528. Work at the National Renewable Energy Laboratory (NREL) was supported by the U.S. Department of Energy, Office of Energy Efficiency and Renewable Energy, and Office of Basic Energy Science, under Contract No. DE-AC36-08-GO28308.

References

[1] P.J. Ferreira, G.J. la O, Y. Shao-Horn, D. Morgan, R. Makharia, S. Kocha, H.A. Gasteiger, Journal of the Electrochemical Society 152 (2005) A2256–A2271.
[2] M.F. Mathias, R. Makharia, H.A. Gasteiger, J.J. Conley, T.J. Fuller, C.J. Gittleman, S.S. Kocha, D.P. Miller, C.K. Mittelsteadt, T. Xie, S.G. Yan, P.T. Yu, Interface 14 (2005) 24–35.
[3] J.F. Wu, X.Z. Yuan, J.J. Martin, H.J. Wang, J.J. Zhang, J. Shen, S.H. Wu, W. Merida, Journal of Power Sources 184 (2008) 104–119.
[4] P. Piela, C. Eickes, E. Brosha, F. Garzon, P. Zelenay, Journal of the Electrochemical Society 151 (2004) A2053–A2059.
[5] H.A. Gasteiger, S.S. Kocha, B. Sompalli, F.T. Wagner, Applied Catalysis B-Environmental 56 (2005) 9–35.
[6] B.C.H. Steele, A. Heinzel, Nature 414 (2001) 345–352.
[7] S.S. Zhang, X.Z. Yuan, H.J. Wang, W. Merida, H. Zhu, J. Shen, S.H. Wu, J.J. Zhang, International Journal of Hydrogen Energy 34 (2009) 388–404.
[8] W. Schmittinger, A. Vahidi, Journal of Power Sources 180 (2008) 1–14.
[9] T.T.H. Cheng, N.Y. Jia, P. He, Journal of the Electrochemical Society 157 (2010) B714–B718.
[10] Y.Y. Shao, J.H. Sui, G.P. Yin, Y.Z. Gao, Applied Catalysis B-Environmental 79 (2008) 89–99.
[11] S.C. Roy, A.W. Harding, A.E. Russell, K.M. Thomas, Journal of the Electrochemical Society 144 (1997) 2323–2328.
[12] S.H. Liu, M.T. Wu, Y.H. Lai, C.C. Chiang, N.Y. Yu, S.B. Liu, Journal of Materials Chemistry 21 (2011) 12489–12496.
[13] B. Choi, H. Yoon, I.S. Park, J. Jang, Y.E. Sung, Carbon 45 (2007) 2496–2501.
[14] Y.G. Chen, J.J. Wang, H. Liu, M.N. Banis, R.Y. Li, X.L. Sun, T.K. Sham, S.Y. Ye, S. Knights, Journal of Physical Chemistry C 115 (2011) 3769–3776.
[15] C.H. Hsu, P.L. Kuo, Journal of Power Sources 198 (2012) 83–89.
[16] F.B. Su, Z.Q. Tian, C.K. Poh, Z. Wang, S.H. Lim, Z.L. Liu, J.Y. Lin, Chemistry of Materials 22 (2010) 832–839.
[17] Y.K. Zhou, R. Pasquarelli, T. Holme, J. Berry, D. Ginley, R. O'Hayre, Journal of Materials Chemistry 19 (2009) 7830–7838.
[18] G. Vijayaraghavan, K.J. Stevenson, Langmuir 23 (2007) 5279–5282.
[19] C.L. Sun, L.C. Chen, M.C. Su, L.S. Hong, O. Chyan, C.Y. Hsu, K.H. Chen, T.F. Chang, L. Chang, Chemistry of Materials 17 (2005) 3749–3753.

[20] Y.K. Zhou, K. Neyerlin, T.S. Olson, S. Pylypenko, J. Bult, H.N. Dinh, T. Gennett, Z.P. Shao, R. O'Hayre, Energy and Environmental Science 3 (2010) 1437–1446.
[21] S. Pylypenko, A. Queen, T.S. Olson, A. Dameron, K. O'Neill, K.C. Neyerlin, B. Pivovar, H.N. Dinh, D.S. Ginley, T. Gennett, R. O'Hayre, Journal of Physical Chemistry C 115 (2011) 13667–13675.
[22] C.H. Wang, H.Y. Dub, Y.T. Tsai, C.P. Chen, C.J. Huang, L.C. Chen, K.H. Chen, H.C. Shih, Journal of Power Sources 171 (2007) 55–62.
[23] R.T. Lv, T.X. Cui, M.S. Jun, Q. Zhang, A.Y. Cao, D.S. Su, Z.J. Zhang, S.H. Yoon, J. Miyawaki, I. Mochida, F.Y. Kang, Advanced Functional Materials 21 (2011) 999–1006.
[24] C.-H. Wang, H.-C. Shih, Y.-T. Tsai, H.-Y. Du, L.-C. Chen, K.-H. Chen, Electrochimica Acta 52 (2006) 1612–1617.
[25] B. Yue, Y.W. Ma, H.S. Tao, L.S. Yu, G.Q. Jian, X.Z. Wang, X.S. Wang, Y.N. Lu, Z. Hu, Journal of Materials Chemistry 18 (2008) 1747–1750.
[26] R.I. Jafri, N. Rajalakshmi, S. Ramaprabhu, Journal of Power Sources 195 (2010) 8080–8083.
[27] R.I. Jafri, N. Rajalakshmi, S. Ramaprabhu, Journal of Materials Chemistry 20 (2010) 7114–7117.
[28] D.C. Higgins, D. Meza, Z.W. Chen, Journal of Physical Chemistry C 114 (2010) 21982–21988.
[29] M.N. Groves, A.S.W. Chan, C. Malardier-Jugroot, M. Jugroot, Chemical Physics Letters 481 (2009) 214–219.
[30] C.K. Acharya, D.I. Sullivan, C.H. Turner, Journal of Physical Chemistry C 112 (2008) 13607–13622.
[31] S. Pylypenko, A. Queen, T.S. Olson, A. Dameron, K. O'Neill, K.C. Neyerlin, B. Pivovar, H.N. Dinh, D.S. Ginley, T. Gennett, R. O'Hayre, Journal of Physical Chemistry C 115 (2011) 13676–13684.
[32] Y.G. Chen, J.J. Wang, H. Liu, R.Y. Li, X.L. Sun, S.Y. Ye, S. Knights, Electrochemistry Communications 11 (2009) 2071–2076.
[33] G. Wu, C.S. Dai, D.L. Wang, D.Y. Li, N. Li, Journal of Materials Chemistry 20 (2010) 3059–3068.
[34] Z.L. Liu, F.B. Su, X.H. Zhang, S.W. Tay, ACS Applied Materials and Interfaces 3 (2011) 3824–3830.
[35] T. Kondo, T. Suzuki, J. Nakamura, Journal of Physical Chemistry Letters 2 (2011) 577–580.
[36] T.S. Olson, A. Dameron, S. Pylypenko, K. Hurst, A. Corpuz, S. Christensen, J. Bult, D.S. Ginley, R. O'Hayre, H.N. Dinh, T. Gennett, Abstracts of Papers of the American Chemical Society 242 (2011).
[37] S. Pylypenko, K. Wood, A. Queen, R. O'Hayre, A. Dameron, T. Olson, K. Hurst, S. Christensen, J. Bult, K. O'Neill, D. Ginley, T. Gennett, H. Dinh, T. Holme, A. Borisevich, K. More, Abstracts of Papers of the American Chemical Society 242 (2011).
[38] This was checked by going through all the Web of Knowledge results for the topic search phrases "durability AND nitrogen doped AND Pt", "Durability AND nitrogen doped AND PtRu", and "stability AND nitrogen doped AND PtRu". Last Checked on Jan 16, 2012.
[39] A.A. Dameron, T.S. Olson, S.T. Christensen, J.E. Leisch, K.E. Hurst, S. Pylypenko, J.B. Bult, D.S. Ginley, R.P. O'Hayre, H.N. Dinh, T. Gennett, ACS Catalysis 1 (2011) 1307–1315.
[40] S.C. Thomas, X.M. Ren, S. Gottesfeld, P. Zelenay, Electrochimica Acta 47 (2002) 3741–3748.
[41] H.A. Gasteiger, N. Markovic, P.N. Ross, E.J. Cairns, Journal of Physical Chemistry 98 (1994) 617–625.
[42] H.N. Dinh, X.M. Ren, F.H. Garzon, P. Zelenay, S. Gottesfeld, Journal of Electroanalytical Chemistry 491 (2000) 222–233.
[43] M. Ahmed, I. Dincer, International Journal of Energy Research 35 (2011) 1213–1228.
[44] J. Aragane, T. Murahashi, T. Odaka, Journal of the Electrochemical Society 135 (1988) 844–850.
[45] J. Aragane, H. Urushibata, T. Murahashi, Journal of Applied Electrochemistry 26 (1996) 147–152.
[46] D.R. Rolison, P.L. Hagans, K.E. Swider, J.W. Long, Langmuir 15 (1999) 774–779.